PROBABILITIES OF HIGH-CONCENTRATION EVENTS IN SCALAR POINT-SOURCE PLUME IN A TURBULENT BOUNDARY LAYER

Miaoyan Pang and Kapil Chauhan*
Centre for Wind, Waves, and Water
School of Civil Engineering, The University of Sydney, Syndey, NSW 2006
*kapil.chauhan@sydney.edu.au

ABSTRACT

In this paper, we study the probability density functions (PDFs) of concentration in a plume of passive scalar released from a point-source in a turbulent boundary layer. The emphasis is on the high concentration events, i.e. the tail of the PDF. Past studies on PDFs have focused on limited positions in the plume, such as at the plume centreline. Peak concentration events are not well-documented either. We extend the analysis of PDFs of the temporal concentration signal and the underlying instantaneous peaks for many locations across the whole plume width. It is found that a Gamma distribution can partly describe the PDFs, i.e. for finite concentration magnitudes, a result that is in agreement with previous studies. A mathematical model for the tail of PDFs for high concentration magnitudes can be simplified with a pure exponential function and the corresponding decay exponents are found to be similar across the plume. A scaling factor is then used to collapse the PDF tails cross the plume. The analysis show that the decay exponents are proportional to the power of plume half-width. On the other hand, the scaling factor has a Gaussian distribution and hence could be related to the mean concentration profile. Therefore, mean concentration profiles could be used to predict the high concentration tails. We also study the tail of the PDFs of peaks over certain threshold and maxima over a period. The tails of these PDFs also share the same decay exponents as that of the full-signal PDFs.

INTRODUCTION

The spread of a plume in a turbulent boundary layer has been extensively studied. However, due to the complexity of the turbulent flow, prediction of the instantaneous concentration downstream of the source cannot be realised. Hence, one has to rely on statistics to *predict* occurrence of instantaneous events with desired certainty, of which high-concentration events are of practical interest. The approach is to use the PDFs of concentration at different points in space as they contain information of all moments as well as the probability of occurrence of extreme events.

Chatwin & Sullivan (1990) highlight the scaling law between the mean concentration and the rms of the concentration from both theory and experimental data for uniform source. They extend their theory to similarity of the ratio of higher-order consecutive moments. However their predictions are not suitable for near field where the concentration fluctuations are highly dependent on the source condition. Their work is complemented by that of Sawford & Sullivan (1995) for near field and background flow of homogeneous turbulence. Since the PDF includes the information of all moments, these studies suggest the possible existence of self-similarity of concentration PDFs.

Various distributions are fitted to concentration data in past studies, including but not limited to Weibull, Beta, Gamma, log-normal, and Gaussian distributions. The results are summarised by (Cassiani *et al.*, 2020, See Table 2). Most researchers have found agreement of the Gamma distribution (Nironi *et al.*, 2015; Efthimiou *et al.*, 2016; Oettl & Ferrero, 2017) with their data, while Yee *et al.* (1993) concludes that a Weibull distribution describes the concentration PDFs better. Hence, there is no broad agreement on a representative functional form. It is to be noted here that these studies attempt to fit the full-signal PDF, which includes near-zero and non-zero concentrations. However, instantaneous concentration of scalar, particularly in a meandering plume, is intermittent, i.e. the concentration is zero for a certain duration and then peaks to values much greater than the mean-concentration at other times. Such concentration behaviour is not suitably represented by a Gamma distribution or a Weibull distribution, which prescribes $p(C=0)=0$. Here C is the instantaneous concentration and p is the probability density function. Therefore when fitting the full range of the concentration PDF, one needs to take into consideration both the possible peak at $C=0$ due to intermittency and the overall shape at $C>0$. Nironi *et al.* (2015) verifies the effect of intermittency, π, by plotting the PDF for signals with various intermittency. Hypothetically, the PDF of a uniform source with no molecular diffusion is

$$p(C;\mathbf{x},t)=\pi(\mathbf{x},t)\delta(C-C_1)+(1-\pi(\mathbf{x},t))\,\delta(C) \quad (1)$$

where C_1 is the source concentration(O'Brien, 1978; Chatwin & Sullivan, 1990). Here the intermittency is accounted for by the Dirac-delta function at $C=0$. When molecular diffusion is present, the first term becomes a probability function

$$p(C;\mathbf{x},t)=\pi(\mathbf{x},t)f(C;\mathbf{x},t)+(1-\pi(\mathbf{x},t))\,\delta(C) \quad (2)$$

where f is the PDF (similar to equation 14 by Chatwin & Sullivan (1989)). In a follow-up study, Yee & Chan (1997) discuss fitting a shifted and clipped-Gamma distribution to the full signal with assumptions that simplify the role of molecular diffusion. By examining the exceedance probability distribution of the data and the model, the higher concentrations are found to be under-predicted.

The tail of PDFs are of interest because high concentration of pollutants are more concerning, whereas low concentration measurements are affected by the instrumentation (Cassiani *et al.*, 2020). High concentration statistics e.g. 90^{th} and

98$^{\text{th}}$ percentile are used in regulations to quantify odour impact (Oettl & Ferrero, 2017; Invernizzi *et al.*, 2020, e.g.). The challenge of modelling the tail of concentration is compounded by unavailability of reliable data as long sampling times are needed. Only a few studies focus on fitting certain distributions to the tail of the PDFs, although the extent of fits vary in each study. Schopflocher (2001) and Mole *et al.* (2008) used Extreme Value Theory to investigate the 'goodness' of fit of a Generalized Pareto Distribution (GPD) for concentration larger than the local mean. The variation of the shape parameter in the GPD cross-plume is found to be relatively constant in Schopflocher (2001). Efthimiou *et al.* (2016) used a Gamma distribution to fit the 75$^{\text{th}}$ to 99$^{\text{th}}$ percentile of the concentration data whereas Oettl & Ferrero (2017) found that a Weibull distribution describes the PDF well when the concentration is higher than the 90$^{\text{th}}$ percentile. Among these three fits, both Weibull and Gamma have a exponential tail while GPD does not. Hence, our goal is to: a) evaluate the appropriate distribution to fit the PDF tails of concentration, and b) assess the variation of the distribution parameters across the plume.

This conference paper briefly describes our initial findings on the parameterisation of the high concentration tails using data from plume released at different source-heights in a turbulent boundary layer.

EXPERIMENTAL DETAILS

A neutrally buoyant gas mixture (1.5% iso-Butylene mixed in 98.5% Nitrogen) is released from a point-source located at different heights in a turbulent boundary layer. Further details of the facility and the experiments can be found in Talluru *et al.* (2017). Simultaneous measurements of velocity and concentration measurements are acquired, however here we are only concerned with the concentration measurements. The instantaneous concentration downstream of the plume source is measured using a Photo-Ionisation Detector (PID) that is sensitive to the iso-Butylene present in the release mixture and has a frequency response of 400 Hz. Multiple acquisitions are made across the plume with a sampling time of 300 sec for each position. The PID is calibrated before and after each experiment to account for background concentration and instrument drift. After applying the calibration technique outlined in Talluru *et al.* (2019*a*), the mean- and rms-concentration profiles are found to agree well with the Gaussian (or Reflected-Gaussian) behaviour that is well-known (Talluru *et al.* (2017, 2018)). However, there is still a $\pm 3\%$ systematic error and $\pm 2\%$ repeatability error (Talluru *et al.*, 2017). Here we will examine the concentration signals when the plume is released at $S_z/\delta = 32/\delta^+, 350/\delta^+, 0.1$, and 0.25, S_z being the source height and $\delta = 0.31$ m being the boundary layer thickness. The measurements are acquired at a distance $S_x = 0.5\delta$, δ, 2δ, and 4δ downstream of the source.

PROBABILITY DISTRIBUTION FUNCTIONS

Although various distributions are used in literature (Cassiani *et al.*, 2020, e.g.) to fit the full-signal PDF of measured concentration, none is appropriate for describing the full range of concentration signal. The quality of the fit, typically assessed by some measure such as the R-square, also depends on the fidelity of the experimental data and the range over which fitting is performed. Most experimental observations indicate that Weibull and Gamma distributions describe the concentration PDFs better. The Gamma distribution is given as,

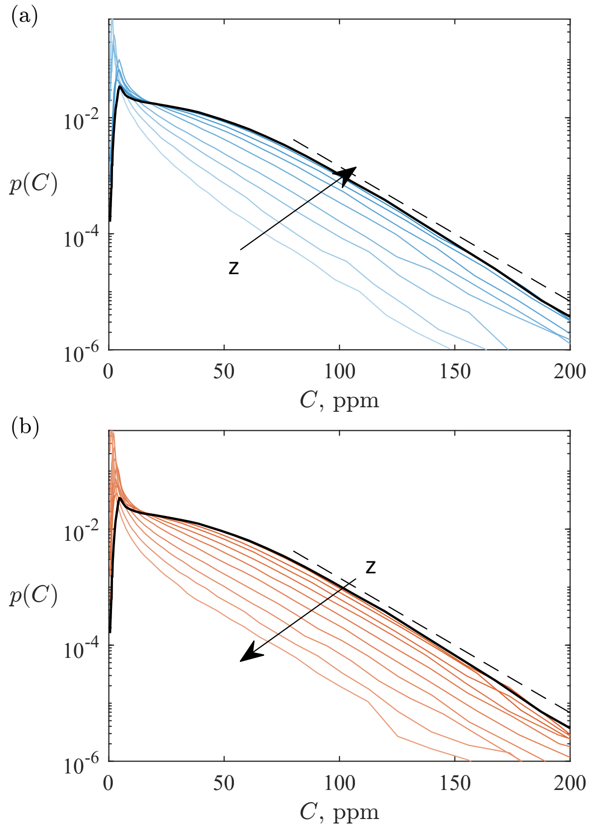

Figure 1. PDFs as a function of the instantaneous concentration, C, for $S_x = 0.1\delta$, $S_z = 1\delta$. The solid black line represents the PDF on the plume centreline and the red lines are the ones above the centreline. The blue lines are the PDFs below the centreline. The exponential behaviour is indicated by the dashed black line.

$$p(C) = \frac{1}{\Gamma(k)\theta^k} C^{k-1} \exp\left(-\frac{C}{\theta}\right), \tag{3}$$

where k is the shape parameter and θ is the scale parameter.

Typically, PDFs of the instantaneous concentration, C, and instantaneous concentration normalised by its r.m.s., $C/\sqrt{\overline{c^2}}$ ($c = C - \overline{C}$, concentration fluctuations), are used as a variable (Nironi *et al.*, 2015; Talluru *et al.*, 2017). Since, $\overline{c^2}$ varies across the plume, to compare the PDFs at two distinct locations within the plume, here we study the PDF of the instantaneous concentration, C.

Figure 1 plots the experimentally determined PDFs for $S_x = 0.1\delta$, $S_z = 1\delta$. The PDF at the plume centreline is shown by the solid black line. PDFs for measurements below the centreline are shown by red lines in figure 1a whereas those for measurements above the centreline are shown by blue lines in figure 1b. It is evident that the high-concentration tails have an exponential behaviour (a straight line on linear – log axes). Moreover, the indicative slope of the tail of each PDF appears to be similar too, i.e. they have similar decay exponent. Also, it is seen that in the vicinity of $C = 0$, the PDFs exhibit a sharp peak due to the presence of near-zero values in the signal resulting from the intermittent nature of concentration in a meandering plume. This peak behaviour near $C = 0$ cannot be modelled by the Gamma distribution, even though it is suitable for higher concentration values. Since the Gamma distribution

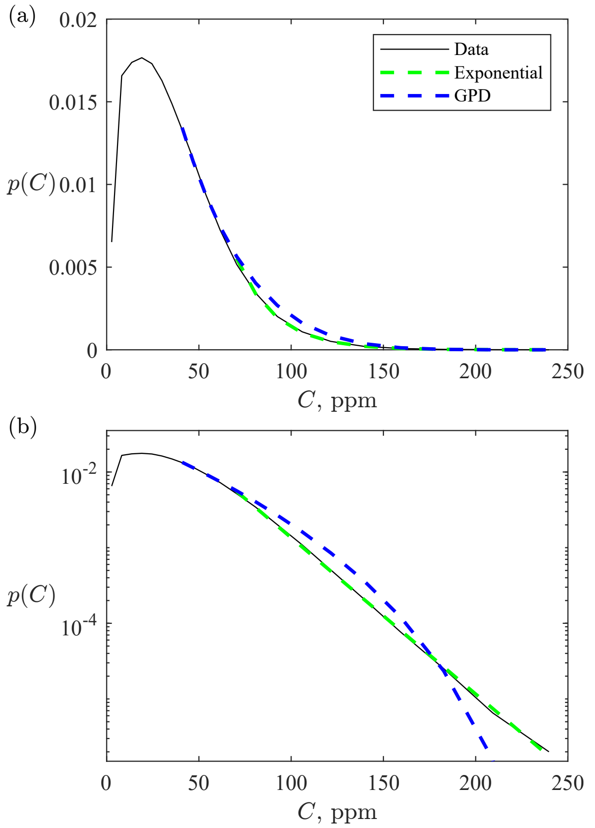

Figure 2. Comparison of Generalized Pareto Distribution and Exponential fits for the PDF tails at the plume centreline for $S_x = 0.1\delta$, $S_z = 1\delta$, on a (a) linear – linear axes (b) linear – log axes.

is characterised by the exponential term in equation 3 at higher concentrations, consistent with the experimental observations, we simplify the fitting to the tail using a purely exponential function given as,

$$p(C) = A \cdot \exp\left(-\frac{C}{\theta}\right), C > C' \quad (4)$$

where C' is arbitrary. Two other studies that particularly focus on the tail of the concentration PDF are by Mole *et al.* (2008) and Schopflocher (2001). They use GPD instead of an exponential function. A GPD fitted to our data as an example is plotted in figure 2. It can be observed that, though the prediction of a GPD seems to be acceptable on a linear – linear plot, it over-predicts in the range of approximately $75 < C < 175$ on a linear – log scale and under-predicts beyond that. Thus its prediction appears to be reasonably good on a linear plot, more stringent examination reveal that the present data is not suitably represented by the GPD. The parameters A and θ in equation 4 are determined using an iterative non-linear least squares method for each PDF and their variation across the plume are shown in figure 1. The decay exponent, θ, is plotted in figure 3a as filled symbols, whereas the coefficient, A is plotted in figure 3(b). It was found that the tail of PDF for wall-normal locations near the edge of the plume on either side have a slightly different decay exponent. This indicates a decreased statistical convergence towards the plume edge (Chatwin & Sullivan, 1990; Yee & Chan, 1997). Based on the above observation, figures 1 and 2 only includes the locations in the plume where $\overline{C} > 0.1\overline{C}_{\max}$, where $\overline{C}_{\max}$ is the mean concentration at plume centreline. It is seen that the decay exponent is almost constant across the plume, indicative of a statistical similarity for high-concentration events. This behaviour of the concentration-tail is analogous to the similarity of concentration-spectra observed by Talluru *et al.* (2019*b*). The median of decay exponents in figure 3(a) is used to plot the dashed line in figures 1a and 1b, indicating that all tails could be modelled using a single θ value. Schopflocher (2001) and Mole *et al.* (2008) also found the shape parameter that they used to fit a GPD to the PDF tail to be constant. Mole *et al.* (2008) argued that the physical reason why the tails has a universal character is due to the velocity field and the molecular diffusion. Further, we note that the distribution of the coefficient A has a Gaussian shape about the plume centreline, as illustrated in figure 3b.

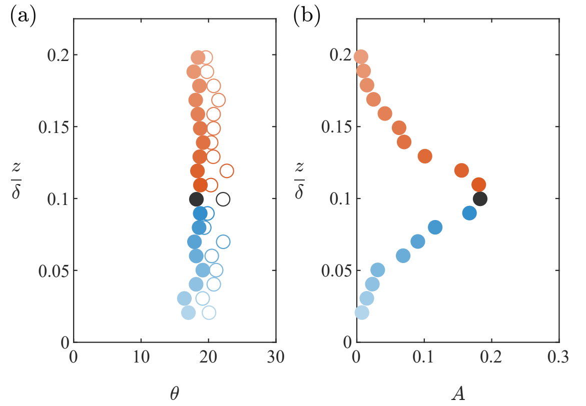

Figure 3. For $S_x = 0.1\delta, S_z = 1\delta$, (a) θ, the decay exponent, from the exponential fit to the high concentration tail of the PDFs. The filled circles are for full-signal PDFs and the empty circles are from PDFs of peaks. (b) Coefficient A for full-signal PDFs.

SPATIAL VARIATION OF PARAMETERS

In this section we extend the analysis to other source distances and source heights. Hereafter, $S_z/\delta = 32/\delta^+$ is referred to as Ground Level Source (GLS) and the other three S_z as Elevated Sources (ES). We find that PDFs of all ES considered here exhibit a near constant behaviour of the decay exponent, θ (as observed in figure 1b, although θ varies for each S_z and S_x combination). This implies that the PDFs of C can be multiplied by a factor such that the tails of the PDFs for each source condition will collapse onto single curve. Here we denote this factor as $1/\mu$. It is obvious that $\mu \equiv A/A_{\text{centreline}}$ from equation 4 and $\mu = 1$ at the plume centreline. Figure 4a shows the resulting PDFs for $S_x = 0.5\delta$ and $S_z = 0.1\delta$ and 4b plots those of $S_x = 4\delta$ and $S_z = 0.1\delta$. Similar to figure 1, the solid black line is the PDF at plume centreline and the dashed black line represents the average slope of tail. Figure 4a and 4b demonstrate the self-similarity of PDF tails and the possibility to develop scaling laws for modelling. A representative decay exponent, θ is determined for plume released from four source distances and four source heights. We then examine the trend of the decay exponent by plotting θ and $\theta_{\max}$, where θ is the mean decay exponent and $\theta_{\max}$ is the decay exponent at the plume centreline. Figure 5 illustrates the relationship between θ and plume half-width calculated from the C_{rms} profile, δ_z, for all ES. Firstly, the values of θ and $\theta_{\max}$ for a given S_z and S_x combination are close, except for those of $S_x = 4\delta$ and $S_z/\delta = 350/\delta^+$ (black diamond symbol). A possible reason

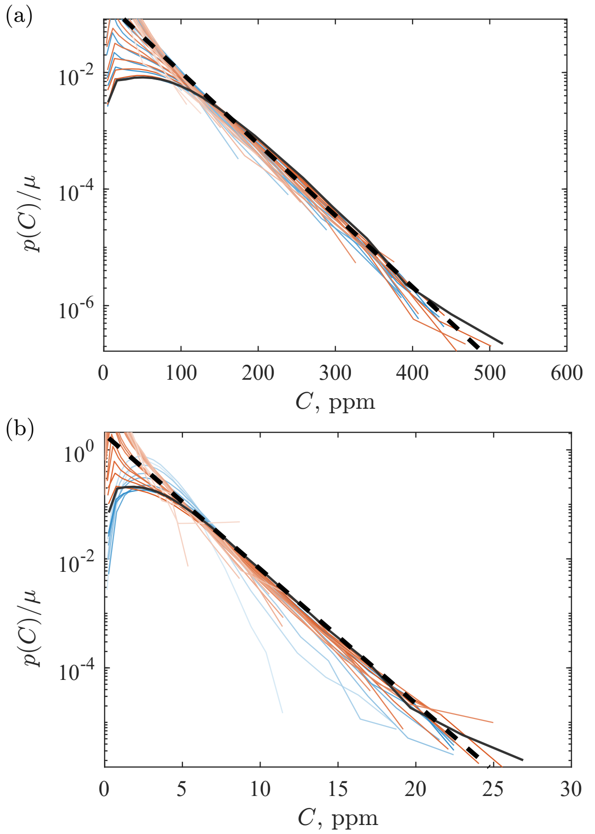

Figure 4. Collapsed PDFs of C for (a) ES $S_x = 0.5\delta$, $S_z = 0.1\delta$. (b) ES $S_x = 4\delta$, $S_z = 0.1\delta$. The collapsed PDFs are obtained by dividing a the original PDF $p(C)$ by μ.

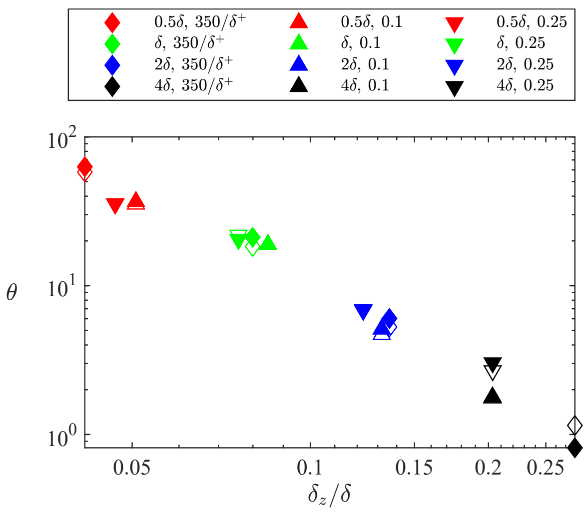

Figure 5. θ vs δ_z (half-plume width) for all ES. The first number in the legend is the source distance, S_x, and the second is source height, S_z/δ. Solid symbols are centreline PDFs and hollow ones are the average slopes for all PDFs.

is that at farther downstream distances from the source, the profile of a lower ES evolves to be similar to that of a GLS. Secondly, it is apparent that θ decreases in the streamwise direction and is proportional to δ_z^B, where B is some exponent. The other parameter in equation 4, A, shows a Gaussian-like behaviour, as plotted in figure 3b. Thus μ is likely to be related to the mean concentration. Figure 6 plots $\overline{C}/\overline{C}_{\text{max}}$ vs μ in a

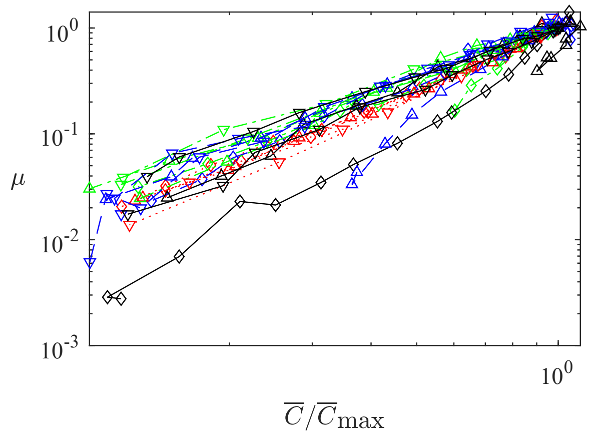

Figure 6. The factor used to collapse $p(C)$, μ, plotted against $\overline{C}/\overline{C}_{\text{max}}$ for all ES. For legend refer to figure 5.

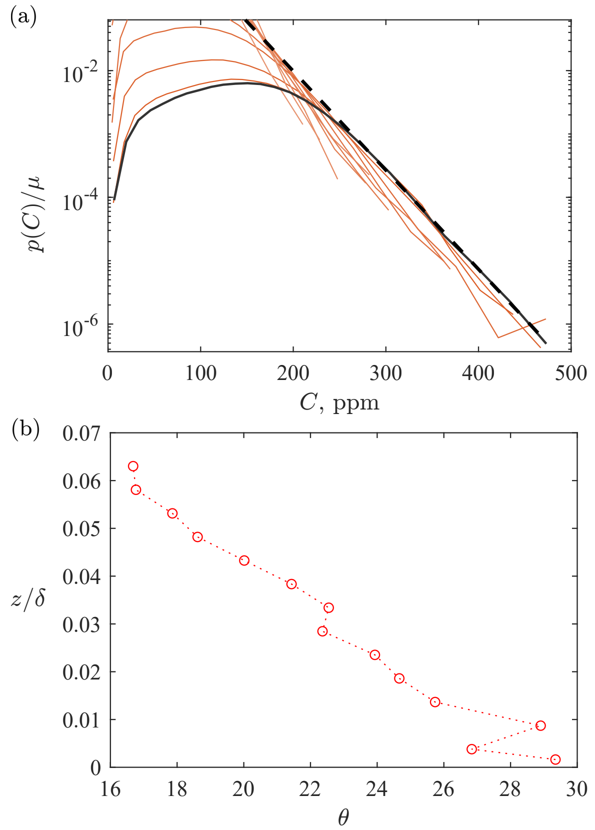

Figure 7. a) Collapsed PDFs of C for a GLS, $S_x = 0.5\delta$, $S_z/\delta = 32/\delta^+$. b)θ calculated for each PDF in the cross-plume direction.

log-log scale for all ES. It is observed that $\mu \propto \left(\overline{C}/\overline{C}_{\text{max}}\right)^D$, where D is some exponent. Again, decreased statistical convergence is observed for $S_x = 4\delta$ and $S_z/\delta = 350/\delta^+$ here (black diamond symbol). In contrast to the above observation, the decay exponent θ varies significantly across the plume for a GLS. The change in slope for each PDF is evident in figure 7a and consequently the PDF tails do not collapse to a single curve after being scaled. Instead the profile of θ for GLS in figure 7b resemble the mean concentration profile for the GLS. We infer that this behaviour of changing decay exponent might be due to wall effect and further analysis is need to characterise this behaviour.

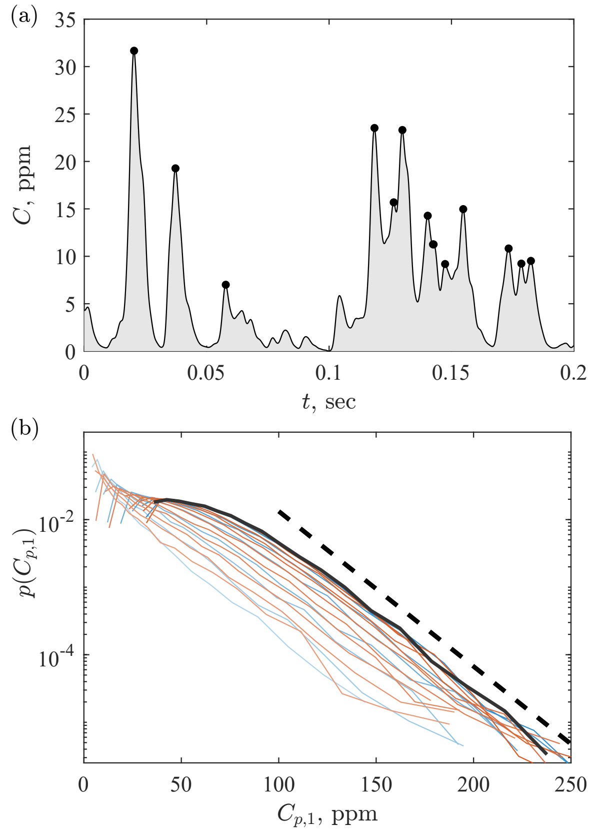

Figure 8. (a) Instantaneous concentration measured for a 0.2-sec period with identified peaks. (b) Probability density functions for peak values only for $S_x = 0.1\delta$, $S_z = 1\delta$.

EXTREME EVENT ANALYSIS

In this section we examine the PDFs for the extreme values in the concentration signal, for which the extreme values are considered to be the local maxima. Two approaches are adopted. First, all local maxima that are above a threshold are examined and second, local maximum over multiple segments of the signal are analysed.

Peak over threshold

Here we determine the local maxima (see figure 8a) in the instantaneous signal at a height z such that the peak values ($C_{p,1}$) are larger than the local mean, $\overline{C}(z)$. The PDFs for these peak values only are plotted in figure 8b and similar to the full-signal PDFs, the PDFs for the peaks also exhibit an exponential behaviour at high concentrations. The decay exponent is evaluated for these PDFs, plotted as hollow symbols in figure 3a, and is close to the values for the full-signal PDFs (solid symbols in figure 3a). We also find that decay exponent for the PDFs of the peaks is nearly constant, evidencing similarity.

Maxima over a period

The probability of maxima in a fixed time-period is commonly studied in meteorology and hydrology, e.g. monthly maxima and annual maxima. Typically, Generalised Extreme Value (GEV) distributions are then fitted for the prediction of extreme events when limited data are available. For example, in wind engineering, the Weibull distribution is more appropriate for the probability distribution of annual maximum wind speed(Holmes & Bekele, 2021). Hence we apply a similar approach to the concentration measurements, where the

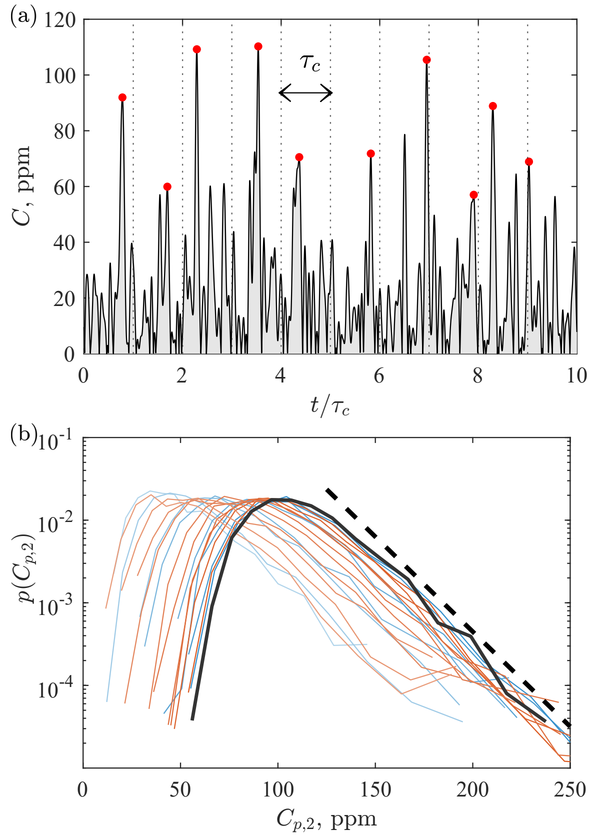

Figure 9. a) Instantaneous concentration measured for a period of 10 time scale for concentration, τ_c, with identified peaks. b) Probability density functions for peak values in each bin for $S_x = 0.1\delta$, $S_z = 1\delta$. The dashed line represents the decay exponent calculated from $p(C)$, in this case, the green triangle in figure 5.

signal at any location is acquired for 300 seconds and thereafter this sampling time is divided into segments of pre-defined duration. We have adopted the pre-defined duration as the time-scale for concentration, τ_c, which is found from the auto-correlation function. The signal is then divided in to segments, each of duration τ_c, and the maximum $C_{p,2}$ from each segment is collected. This method is demonstrated in figure 9a. The PDFs of $C_{p,2}$ are plotted in figure 9b. As anticipated, these PDFs also have an exponential tail, with a decay exponent similar to that for $p(C)$ and $p(C_{p,1})$ in figures 1 and 8b, respectively.

Summary

The results presented here arise from extensive measurements and thus bring in new information to the already extensive literature on PDFs for scalar concentration. The PDFs of concentration measured for varying source heights and source distances exhibit statistical similarity across the plume. We have presented evidence for the decay exponents to be invariant across the plume through the PDFs for $p(C)$, $p(C_{p,1})$, and $p(C_{p,2})$. A novel finding is in the fact that the decay exponent is related to the plume half-width.

The spread of passive scalar is dominated by two mechanisms: turbulent mixing and molecular diffusion (Gifford, 1959). Large concentration events in the plume are thought to reside on thin *strands* or *sheets* and caused by local turbulence (Yee & Chan, 1997). Molecular diffusion is also significant for these high concentration patches due to locally high spatial gradient. Given that the plume width relative to the boundary layer thickness is small, the influence of the local turbulence would be for the whole plume. Thus the two mechanisms for the spread of concentration are persistent across the plume resulting in high concentration events having the same decay exponent in the corresponding PDFs.

Here we have only studied the high-concentration tail of the PDFs and thus the behaviour of low-level concentration is not examined. The analysis is not aimed towards describing the full range of concentration fluctuations, as typically done on past studies. The exponential tail of the PDFs is undoubtedly evident in our measurements, possible due to the long sampling times. This behaviour can thus suggest the appropriate function form for the full-scale PDF, e.g. the Gamma distribution asymptotes to an exponential behaviour for large concentrations. Similar observations have been made by Schopflocher (2001). Although it should be noted that the exponential distribution also results in finite probability, no mater how small, for concentration magnitudes that are above the source concentration. This is unrealistic due to the ever present molecular diffusion. However a possible application is to model the 90$^{\text{th}}$ and 99$^{\text{th}}$ percentile, C_{90} and C_{99}, which are studied in Fackrell & Robins (1982) and Efthimiou *et al.* (2016).

Efforts are also ongoing to reconcile the observations made for concentration PDFs in this paper with the results for the concentration spectra by Talluru *et al.* (2019*b*) and the phenomenological model for the role of large-scale velocity structures by Talluru *et al.* (2018). As such, we have not yet parameterised these statistical variations (particularly for figures 5 and 6) to model the probability or for predictions.

Acknowledgements

The first author would like to thank Dr Murali Krishna Talluru for valuable insights and suggestions. The authors are also thankful to the reviewer(s) who suggested the inclusion of PDFs for extreme events in the analysis presented here.

REFERENCES

Cassiani, M., Bertagni, M.B., Marro, M. & Salizzoni, P. 2020 Concentration fluctuations from localized atmospheric releases. *Boundary-Layer Meteorology* **177** (2-3), 461–510.

Chatwin, P. C. & Sullivan, Paul J. 1989 The intermittency factor of scalars in turbulence. *Physics of Fluids A* **1** (4), 761–763.

Chatwin, P. C. & Sullivan, P. J. 1990 A simple and unifying physical interpretation of scalar fluctuation measurements from many turbulent shear flows. *Journal of Fluid Mechanics* **212**, 533–556.

Efthimiou, G. C., Andronopoulos, S., Tolias, I. & Venetsanos, A. 2016 Prediction of the upper tail of concentration distributions of a continuous point source release in urban environments. *Environmental Fluid Mechanics* **16** (5), 899–921.

Fackrell, J. E. & Robins, A. G. 1982 Concentration fluctuations and fluxes in plumes from point sources in a turbulent boundary layer. *Journal of Fluid Mechanics* **117** (1), 26.

Gifford, F. 1959 Statistical roperties of a fluctuating plume dispersion model. *Advances in Geophysics* **6**, 117–137.

Holmes, J. D. & Bekele, S. 2021 Prediction of design wind speeds and structural safety. In *Wind Loading of Structures*, chap. 2, pp. 40–64. Milton: Taylor & Francis Group.

Invernizzi, M., Brancher, M., Sironi, S., Capelli, L., Piringer, M. & Schauberger, G. 2020 Odour impact assessment by considering short-term ambient concentrations: A multi-model and two-site comparison. *Environment International* **144** (June), 105990.

Mole, N., Schopflocher, T. P. & Sullivan, P. J. 2008 High concentrations of a passive scalar in turbulent dispersion. *Journal of Fluid Mechanics* **604**, 447–474.

Nironi, C., Salizzoni, P., Marro, M., Mejean, P., Grosjean, N. & Soulhac, L. 2015 Dispersion of a passive acalar fluctuating plume in a turbulent boundary layer. Part I: velocity and concentration measurements. *Boundary-Layer Meteorology* **156** (3), 415–446.

O'Brien, E. E. 1978 Stochastic properties of scalar quantities advected by a non-buoyant plume. *Journal of Fluid Mechanics* **89** (2), 209–222.

Oettl, D. & Ferrero, E. 2017 A simple model to assess odour hours for regulatory purposes. *Atmospheric Environment* **155**, 162–173.

Sawford, B. L. & Sullivan, P. J. 1995 A simple representation of a developing contaminant concentration field. *Journal of Fluid Mechanics* **289**, 141–157.

Schopflocher, T. P. 2001 An examination of the right-tail of the PDF of a diffusing scalar in a turbulent flow. *Environmetrics* **12**, 131–145.

Talluru, K. M., Hernandez-Silva, C. & Chauhan, K. A. 2019*a* A robust calibration technique for concentration measurements using ionisation detectors. *Measurement Science and Technology* **30** (7).

Talluru, K. M., Hernandez-Silva, C., Philip, J. & Chauhan, K A. 2017 Measrements of scalar released from point sources in a turbulent boundary layer. *Measurement Science and Technology* **28**, 1–13.

Talluru, K. M., Philip, J. & Chauhan, K. A. 2018 Local transport of passive scalar released from a point source in a turbulent boundary layer. *Journal of Fluid Mechanics* **846**, 292–317.

Talluru, K. M., Philip, J. & Chauhan, K. A. 2019*b* Self-similar spectra of point-source scalar plumes in a turbulent boundary layer. *Journal of Fluid Mechanics* **870**, 698–717.

Yee, E. & Chan, R. 1997 A simple model for the probability density function of concentration fluctuations in atmospheric plumes. *Atmospheric Environment* **31** (7), 991–1002.

Yee, E., Wilson, D. J. & Zelt, B. W. 1993 Probability Distributions of Concentration Fluctuations of a Weakly Diffusive Passive Plume in a Turbulent Boundary Layer. *Boundary-Layer Meteorology* **64**, 321–354.